Proceedings of the 9th U.S. National and 10th Canadian Conference on Earthquake Engineering
Compte Rendu de la 9ième Conférence Nationale Américaine et
10ième Conférence Canadienne de Génie Parasismique
July 25-29, 2010, Toronto, Ontario, Canada • Paper No 1099

IMPROVEMENT IN SEISMIC CONFIGURATION OF SLENDER REINFORCED CONCRETE WALL PIERS ON ISOLATED FOOTINGS

K. Dasgupta[1] and C. V. R. Murty[2]

ABSTRACT

In the current seismic design practice, capacity design of slender Reinforced Concrete (RC) wall piers without enlarged boundary elements and on shallow footing considers plastic hinge to occur at the base along with prevention of other modes of failure during strong earthquake shaking. However, the re-entrant corner of wall pier-footing junction makes it vulnerable to significant damages during strong earthquake shaking. This may require costly seismic retrofitting of bridge footing after every earthquake.

The present study investigates a new geometric configuration at wall pier-footing junction concerned with smooth flow of forces from the pier to the footing. A wall pier from a continuous bridge is provided with linear and curvilinear tapered configurations at the bottom. Linear elastic finite element analysis is carried out in SAP2000 program using 8-noded solid elements for modeling both the wall pier and the footing, and smeared spring elements for soil flexibility. Actual vertical forces and maximum possible lateral forces are estimated during the formation of plastic hinge at the base of the wall pier. Under these forces, the proposed wall pier-footing system exhibits rigid block-type behaviour irrespective of soil flexibility. It is observed that curvilinear taper with a particular profile ensures the most favorable stress distribution and prevents damage in footing below ground level. The region of damage is located above the tapered region and this can be located above normal ground level.

Strategies are presented to suitably proportion the tapered wall pier-footing portion. These strategies are based on three criteria, namely (a) geometry of the curvilinear taper, (b) bearing failure of the underlying soil, and (c) length of footing in contact with the soil. In most of the cases, bearing failure criterion of soil governs the dimensioning of the wall pier-footing system. The detailed parametric study shows the necessity of stress-based design philosophy of tapered wall pier-footings.

[1]Assistant Professor, Department of Civil Engineering, Indian Institute of Technology Guwahati, Guwahati 781039, India, kaustubh.dasgupta@gmail.com

[2]Professor, Department of Civil Engineering, Indian Institute of Technology Hyderabad, Yeddumailaram 502025, India, cvrm@iith.ac.in

Introduction

RC slender structural wall pier is an important component of lateral force resisting system of bridge and viaduct systems. During strong earthquake shaking, formation of plastic hinge at the bottom of the pier is associated with irregular stress distribution and force flow in that region. This has been observed in case of hollow rectangular piers also (Hines and Seible 2004). For wall pier on isolated footing, the geometry of pier-footing junction significantly influences the flow of forces from wall to footing. In the footings, either without any taper from the edge of footing to the edge of the pier or with marginal taper, reentrant corner of pier-footing junction causes severe stress concentration. This is likely to cause local failures of pier-footing junction region and footing.

Past studies on seismic response of wall-piers have focused on out-of-plane failure (Abo-Shadi et al. 2000), vulnerability assessment (Bignell et al. 2005) and applicability of dynamic lattice model (Miki et al. 2002). The analytical behavior of pier-footing has been investigated with Winkler springs at the bottom (Chen and Lai 2003). Strut-and-tie model of footing has been studied in case of bridge columns (Xiao et al. 1996) but not for bridge wall-piers.

In this study, a new geometric configuration is proposed, in wall piers without enlarged boundary elements, to ensure smooth flow of forces at the bottom region and minimise seismic damage in the footing. A detailed parametric study is carried out and possible strategies of proportioning discussed.

Wall Pier Details

A slender RC wall-pier is considered in the present study with aspect ratio of structural walls A_r (= H_w/L_w) as 4.0, where H_w and L_w are height and length of wall pier (Fig. 1). The thickness of the wall pier t_w is taken as 0.2 m uniformly throughout its height. The length L_f, width B_f and thickness t_f of footing are taken as 7.0 m, 1.2 m and 1.35 m respectively. The grades of concrete and steel are taken as M40 and Fe415 respectively. Design lateral force on the wall pier for seismic load case is obtained as per the relevant Indian Code of Practice for highway bridges, namely IRC:6 (IRC:6 2000) for a span of 40 m; the seismic force is obtained for the most severe seismic zone V as per the Indian seismic zoning map.

Isolated wall pier-footings are modeled using 8-noded solid elements in computer program SAP2000 (CSI 2009) with incompatible bending modes option. Characteristic mesh size of 0.1 m was determined from mesh convergence studies (Dasgupta 2008). Linear elastic analysis is carried out under combined vertical and lateral loads expected during actual earthquake shaking. Nodal shear and principal compressive stress demands, τ and $\sigma_{com,p}$ respectively, are monitored in the bottom D-region. These are normalised with respect to average shear stress τ_{av} in wall pier, and bending compressive stress σ_{bot} at bottom of footing respectively. Compression strut angles θ are normalised with respect to 90°.

The behavior of isolated wall-footing is investigated under concentrated vertical and lateral forces with the translational degrees of freedom (DOF) are restrained at the bottom face of footing. The reentrant corner at the wall pier-footing junction tends to draw maximum force under the applied loads, and this leads to severe shear stress concentration (Fig. 2a). In footing, peak τ is observed at the bottom vertically below wall pier-footing junction (Fig. 2b). Variations of longitudinal stress in footing and principal compressive stress at wall pier-footing junction show possibility of flexural-shear cracking and compression failure of concrete respectively

(Dasgupta 2008). Thus, the footing requires inspection and possible strengthening after every earthquake; these may be costly and inconvenient.

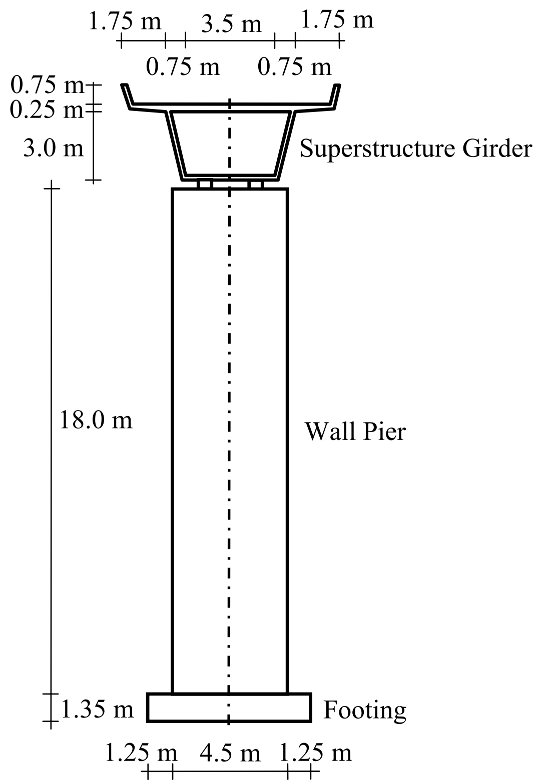

Figure 1 Elevational details of RC wall pier along with superstructure girder section considered in the study.

Parametric Study

Based on results of preliminary study mentioned above, two different tapered configurations are investigated, namely (a) curvilinear profile with degree of curve $n_d \geq 1.0$ (Fig. 3a), and (b) combined taper consisting of linear and curvilinear profiles (Fig. 3b). In case (a), the geometry is defined by a single curve over height of taper H_t and in case (b), by the ratio r_t (=H_{tl} /H_{tc}), where H_{tl} and H_{tc} are the heights of linear and curvilinear profiles.

Critical section of design in tapered wall pier is taken at a distance of idealised plastic hinge length L_p above the top of taper (Figs. 4a and 4b); L_p is taken as $0.5L_w$ (Priestley et al. 1995). Design and detailing are carried out against forces and moments at the critical section (IRC:21 2000). Based on constant overstrength moment capacity M_Ω over L_p and design base shear V_B at the top of wall pier, V is estimated as,

$$V = M_\Omega V_B / M_D, \quad (1)$$

where M_D is the design bending moment. V is applied at the top of wall pier (Fig. 3c) along with unfactored vertical force $P_{ov,ext}$. Variation of $P_{ov,ext}$ during earthquake shaking is not considered.

Soil flexibilities along vertical, in-plane and out-of-plane directions are modeled by smeared springs at the bottom face of footing (CSI 2009). Along the vertical direction, modulus of subgrade reaction below rectangular footing k_{sub} is obtained from ultimate bearing capacity of

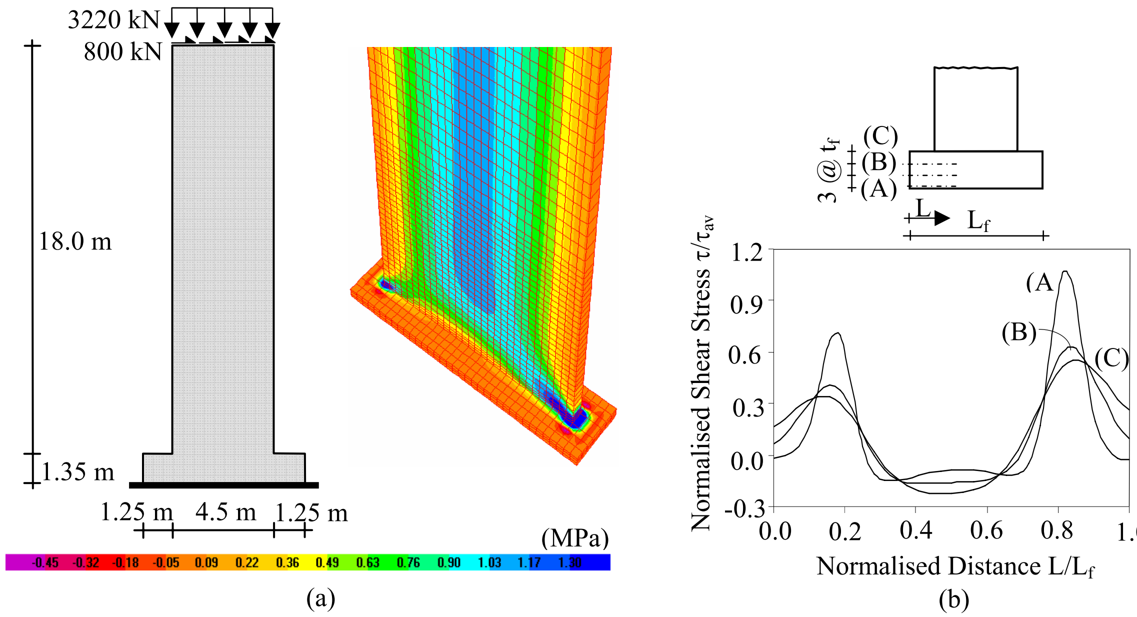

Figure 2 Loads on wall pier and shear stress contours in wall pier and footing, and (b) shear stress demand in footing

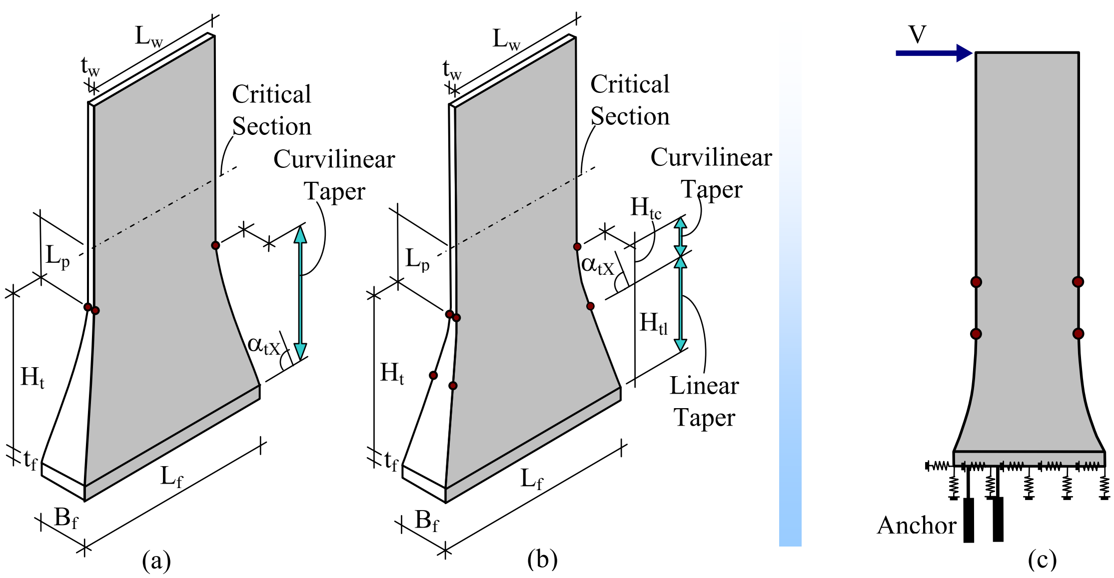

Figure 3 RC wall piers with (a) curvilinear and (b) combined tapered configurations; (c) applied forces during overstrength

soil σ_{bc} and maximum vertical deflection τ_{max} below the toe of footing. Along the other directions, k_{sub} is considered as 25% of the value in vertical direction (Das 1999). Soil anchors are required at suitable locations to reduce uplift and mobilise flexural strength under estimated $P_{ov,ext}$ and V (Fig. 3c). At those locations, vertical translational nodal DOFs are restrained at the bottom face. Absence of overhang in tapered geometry causes rigid block-type behavior of wall pier-footings and linear vertical displacement profiles in all types of soils (Fig. 4a). Consequently, shear stresses are observed to be independent of soil flexibility (Fig. 4b). Uniform variation of stress demand is obtained with increasing in-plane angle of taper α_{tX}. Subsequent analyses are carried out with properties of dry dense sand as strong soil (Dasgupta 2008). Passive pressure of backfill and soil compressibility are not considered in the analyses.

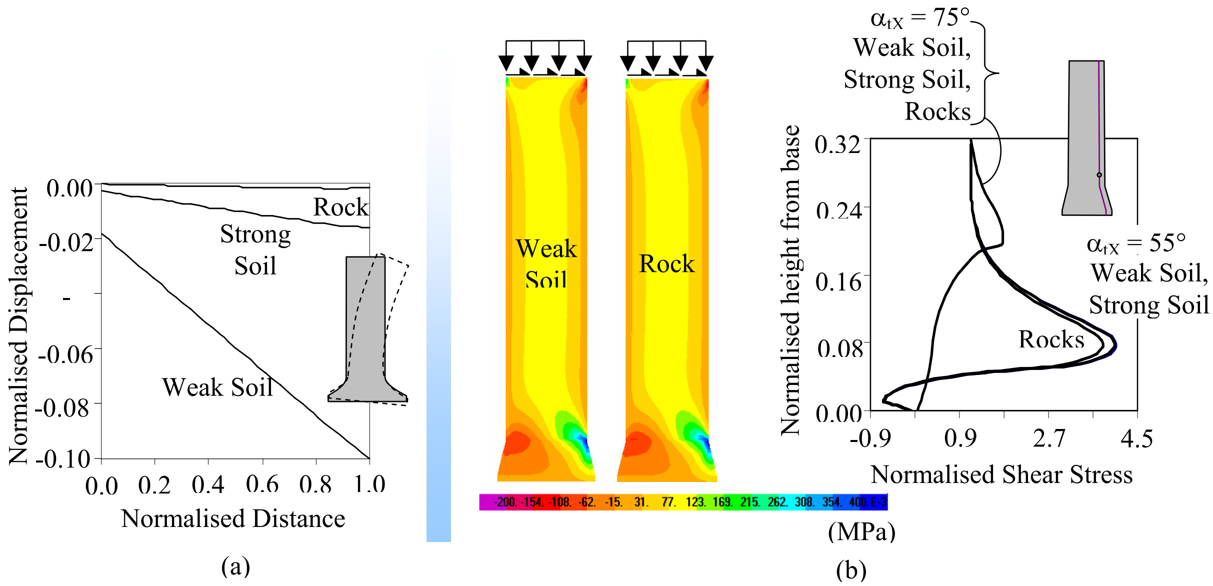

Figure 4 (a) Vertical displacement profile at the bottom; (b) averaged shear stress contours, and vertical shear stress distribution near the edges of wall pier-footings

Configuration

In the investigation of wall-pier configuration, L_w, H_w, t_w, t_f and H_t are kept constant. The investigated wall pier-footings consist of (a) curvilinear tapers with degrees n_d of curve as 1.0, 1.25, 1.5, 1.75, 2.0 and 3.0, and (b) combined tapers with linear profile followed by curves of n_d = 1.5, 2.0 and 3.0 respectively. In wall piers with combined taper, α_{tX} becomes the starting angle of taper at the bottom (Fig. 3b); thus, it depends on taper ratio r_t. Shear stress demand τ is monitored along a curve located at a distance of t_w inside the tapered edge and in central vertical plane of the wall pier. In wall pier-footing with linear taper, τ increases steeply below the transition point due to stress concentration at the re-entrant corner. With increasing n_d, profiles tend to take the shape of footings with sharp re-entrant corners, and intensity of τ increases towards the edges (Fig. 5a). The beneficial characteristics of wall piers with linear taper (i.e., reduction of damage at bottom) and higher n_d (i.e., low τ in transition region) are combined in wall pier-footings with combined taper. Combined taper of n_d = 1.0 and 2.0 is selected for further investigations because this combination eliminates stress concentration in the transition region and performs reasonably well at the bottom region. Comparison of shear stress demands along the edges of tapered wall-footing and wall-footing without taper shows significant reduction of shear stress demand with the use of taper (Fig. 5b). The tapered footing allows a gradual increase of cross-sectional area of the wall towards the bottom, thus removing the stress concentration resulting from the reentrant corner of wall-footing without taper.

In the investigation of influence of r_t on wall pier response, wall piers are analysed with r_t = 0.5, 1.0, 2.0, 3.0 and 4.0. The in-plane and out-of-plane angles of taper, α_{tX} and α_{tY}, are obtained from slope continuity (Dasgupta, 2008). Lower r_t limits the ease and economy of construction of bottom linear taper. With increasing r_t, the location of peak τ near tapered edge shifts upwards (Fig. 5c). Towards the bottom of the footing, maximum difference of 49% is observed in τ between wall piers of low and high r_t because of stress concentration in wall piers with low r_t. Although τ in wall piers with high r_t increases by 37% to that in wall piers with low r_t towards the top of the taper, location of peak demand near ground level makes it a favorable option. From functional point of view, high r_t increases obstruction of space on the sides of wall pier due to more flaring of linear taper. This drawback of high r_t is not significant because most of the tapered portion is proposed to be below ground level. Thus, r_t of 3.0 is chosen in the present study.

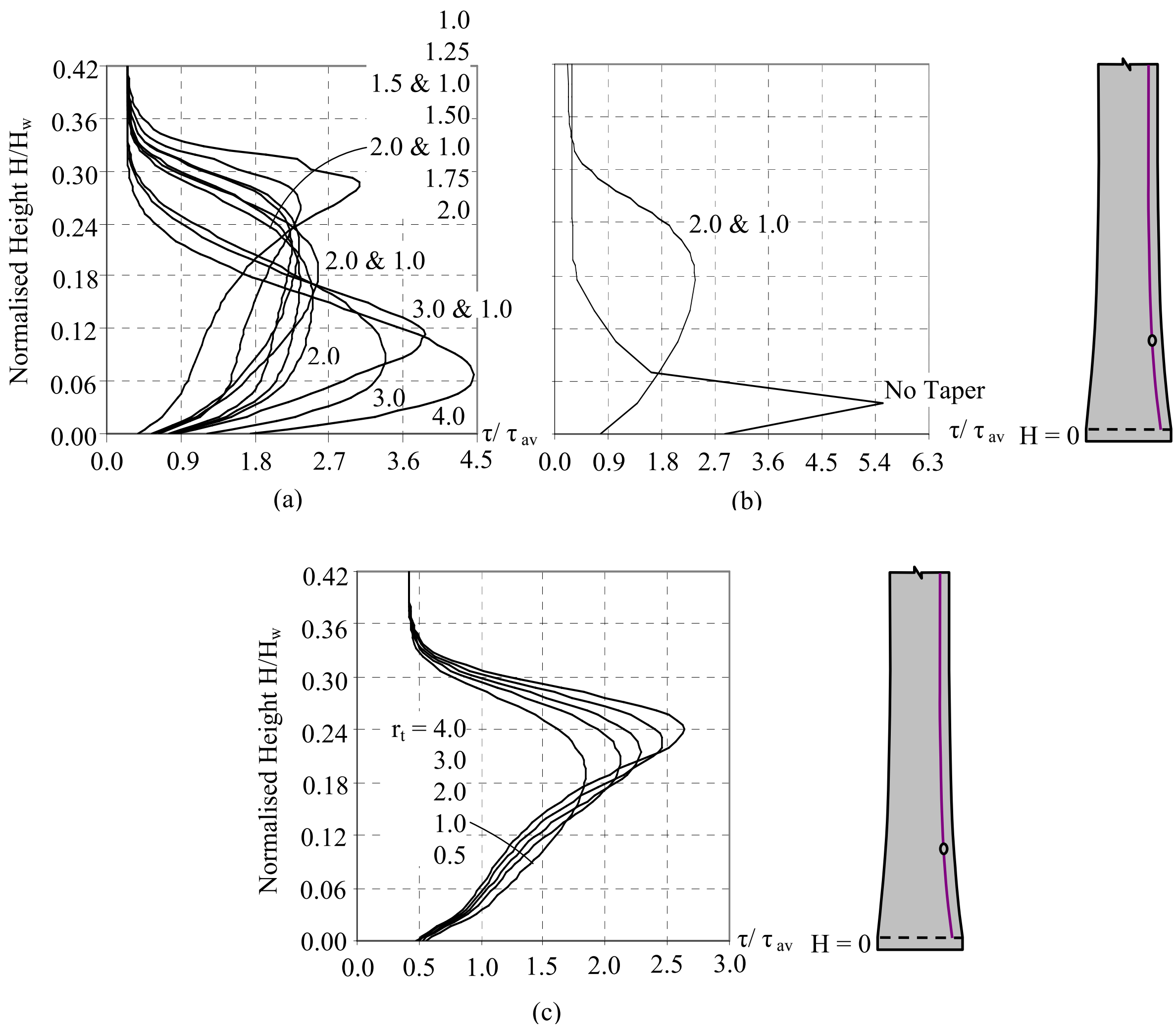

Figure 5 (a) Variation of shear stress demand with degree of taper; (b) comparison of shear stress demand for walls with and without taper and (c) variation of shear stress demand with taper ratio

Two new parameters are introduced to characterise the geometry of combined taper, namely (a) length factor α_L (= L_w/L_f), and (b) width factor α_w (= t_w/B_f). For a particular α_L and other geometric parameters, limits on α_{tX} are derived for three different criteria, namely (a) slope continuity of curvilinear taper, (b) contact of wall pier-footing with underlying soil (full or partial contact), and (c) maximum bearing pressure of soil below wall pier-footing not exceeding σ_{bc} (Dasgupta 2008). The influence of α_L is investigated here.

Length Factor

Higher α_L leads to lower L_f and overall economy of construction of tapered wall pier-footings; here, wall pier-footings are analysed with length factors α_L = 0.6, 0.7, 0.8 and 0.9 under the combined $P_{ov,ext}$ and V. Tapered geometry of wall pier with lower α_L causes concentration of τ (Fig. 6a), with almost 70% reduction in τ between wall piers with α_L as 0.6 and 0.9. In the bottom central region of wall-pier, negative shear stresses increase with α_L because of reduction in the available wall pier sectional area. The principal compressive stress $\sigma_{com,p}$ does not show significant variation in the edge region (Fig. 6b). Local strengthening of the wall pier-footing is required to account for the irregular variation of τ at anchor locations (Dasgupta 2008). Higher α_L leads to lower cost of construction and τ in transition region. Distribution of τ becomes more irregular towards the bottom with higher α_L, and this increases its vulnerability to seismic damage. Thus, selection of α_L is a trade-off between the two.

Stress demands τ and $\sigma_{com,p}$ are compared with design shear strength τ_c and design flexural compressive strengths $\sigma_{b,com}$ of concrete respectively. Shear failure of concrete is expected in the tapered region (Fig. 6a) because of low τ_c arising from design longitudinal steel requirement. Compression failure of concrete at design level is not expected in the tapered region (Fig. 6b). Considering the trade-off between demand and ease of construction and the extent of damage at the bottom, recommended length factor of slender wall pier-footing is 0.7.

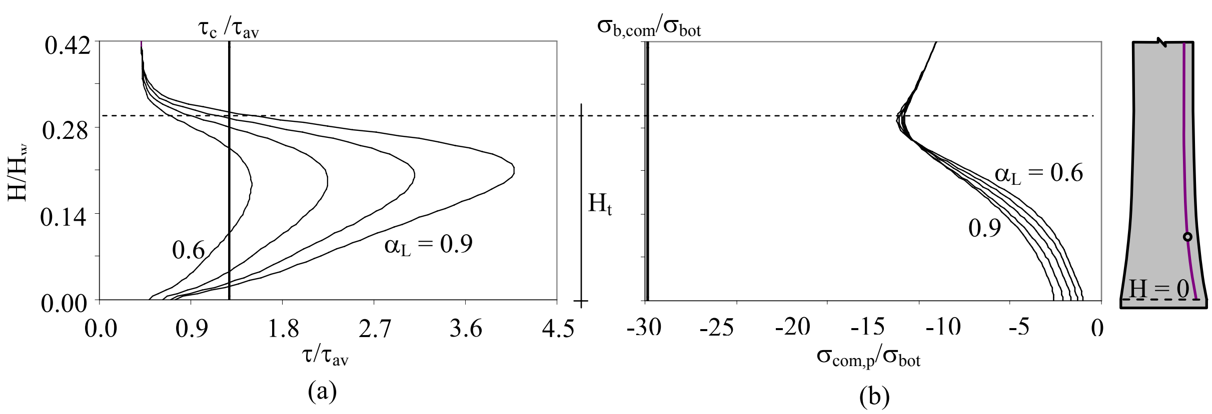

Figure 6 Variation of stress demand and design strength with length factor for (a) shear and (b) principal stresses near the tapered edge in the central vertical plane of wall pier

Angle of Taper

In RC wall pier-footing, direction of force flow at any point is given by angle of compression strut θ. At any point it is obtained as the inclination of principal compressive stress with the horizontal. Under concentrated vertical compression $P_{ov,ext}$ and lateral force V, the possible range of θ is $45° \leq \theta \leq 90°$. Under the combined action of distributed $P_{ov,ext}$ and V, the proposed angle θ_p in the bottom region is given as

$$\theta_p = \pi/4 + 0.5\tan^{-1}(P_{ov,ext}/V), \quad (2)$$

where $P_{ov,ext}$ is the unfactored vertical compression, and V overstrength shear demand at the critical section of the wall pier. With increase in α_L (i.e., decrease in L_f), force flow tends to get concentrated towards the anchor locations. Also, in wall pier with low α_L more length of footing is available for forces to spread out. In the tapered region, the proposed estimate θ_p is observed to be more than minimum strut angle θ_{min} for $\alpha_L = 0.7$ (Fig. 7); thus, θ_p may be considered as a measure of θ_{min}. Under different combinations of $P_{ov,ext}$ and V, α_{tX}/θ_p is observed to exceed θ_{min}/θ_p (Dasgupta 2008) in the bottom region for most of the α_L. Also, the range of variation of α_{tX}/θ_p is 0.9-1.0. Thus, α_{tX} may be estimated by Eq. 2. Further investigations are required of possible modification of Eq. 2 to account for inelastic wall pier response during earthquakes.

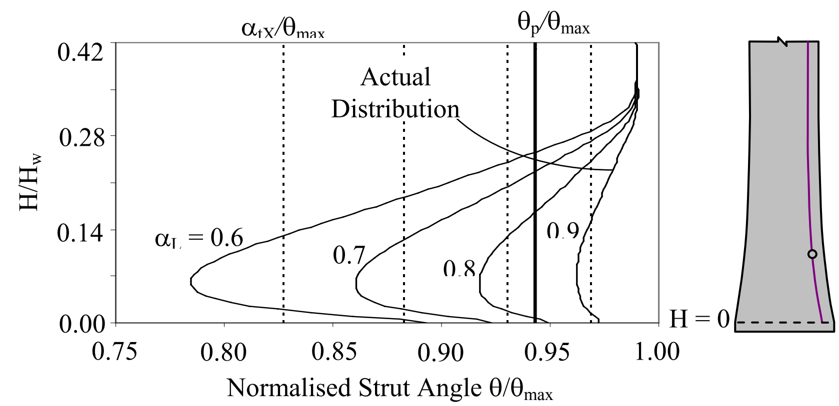

Figure 7 Comparison of proposed and actual strut angle distribution in tapered wall-footing

Construction

Construction of tapered RC slender wall pier-footing involves construction of prefabricated tapered portion and straight vertical portion at site. To continue casting of straight portion, longitudinal reinforcement need to extend upto a distance of $1.5L_p$ above the top of precast portion; thus, splicing of reinforcement is eliminated in the inelastic region (Fig. 8). Splicing of bars may be permitted beyond a height of $1.2L_p$ above the top of tapered portion. Possible erection points, for lifting and placing the unit, may be located at the top surface, and lifting hooks attached at those locations. These are not shown in Fig. 8.

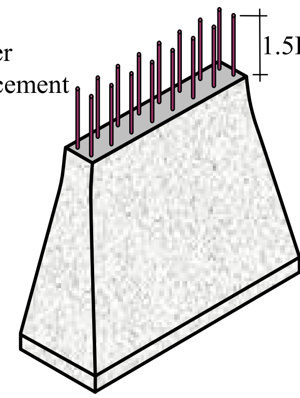

Figure 8 Precast tapered portion in RC wall pier-footing without enlarged boundary elements

Conclusions

The following salient conclusions can be drawn from the study:

(a) Combination of second order elliptic and linear tapers gives favorable stress response in the tapered region of slender wall piers. The ratio of heights of linear to elliptic taper is recommended as 3.0.
(b) Tapered wall pier-footings are expected to be in partial contact with the underlying soil during strong earthquake shaking.
(c) The length factor of slender wall pier-footings is recommended as 0.7 for reasonable stress response.
(d) In wall pier-footings under unfactored vertical compression $P_{ov,ext}$ and overstrength shear demand V, the starting angle of taper may be estimated as $\theta_p = \pi/4 + 0.5\tan^{-1}(P_{ov,ext}/V)$.
(e) The region of seismic damage in slender wall pier-footings is shifted above the tapered region. The height of taper may be suitably chosen to determine the location of damage.
(f) Seismic damage in tapered region of slender RC wall pier can be achieved by making (i) maximum principal tensile stress to be significantly less than the cracking strength of concrete, and (ii) maximum principal compressive stress to be less than the design compressive strength.

Further inelastic analyses of slender wall pier-footings need to be carried out in order to investigate the behavior under strong earthquake shaking.

Acknowledgement

The authors gratefully acknowledge the financial support received from Ministry of Human Resource Development of the Government of India in carrying out the research work.

References

Abo-Shadi, N. A., M. S. Saiidi and D. H. Sanders, 2000. Out-of-Plane Seismic Response of Reinforced Concrete Bridge Pier Walls, *ACI Structural Journal* 97 (6), 803-813.

Bignell, J. L., J. M. LaFave and N. M. Hawkins, 2005. Seismic Vulnerability Assessment of Wall Pier Supported Highway Bridges using Nonlinear Pushover Analysis, *Engineering Structures* 27 (14), 2044-2063.

Chen, X. -C., and Y. -M. Lai, 2003. Seismic response of bridge piers on elasto-plastic Winkler foundation allowed to uplift, *Journal of Sound and Vibration*, 266 (5), 957-965.

CSI, 2009. *SAP2000: Integrated finite element analysis and design of structures*, Computers and Structures Inc., California, USA.

Dasgupta, K., 2008. Improvement in geometric design of reinforced concrete structural walls to resist earthquake effects. *PhD Thesis*, Indian Institute of Technology Kanpur, India.

Das, B. M., 1999. *Principles of foundation engineering*, Brooks/Cole Publishing Co., California, U.S.A.

Hines, E. M., and F. Seible, 2004. Web Crushing Capacity of Hollow Rectangular Bridge Piers, *ACI Structural Journal*, 101 (4), 569-579.

Hsu, Y. T., and C. C. Fu, 2000. Study of Damaged Wushi Bridge in Taiwan 921 Earthquake, *Practice Periodical on Structural Design & Construction, ASCE*, 5 (4), 166-171.

Miki, T., J. Niwa and M. Lertsamattiyakul, 2002. Numerical Evaluation for Seismic Performance of Reinforced Concrete Bridge Piers Using Dynamic Lattice Model. *Journal of Materials, Concrete Structures and Pavement, JSCE*, 704 (55), 151-161.

Xiao, Y., M. J. N. Priestley and F. Seible. 1996. Seismic Assessment and Retrofit of Bridge-Column Footings. *ACI Structural Journal*, 93 (1), 79-94.

Priestley, M. J. N., F. Seible and G. M. Calvi, 1995. *Seismic Design and Retrofit of Bridges,* John Wiley & Sons Inc., USA.

IRC:6-2000, (2000), Standard Specifications and Code of Practice for Road Bridges. Section: II, Loads and Stresses (Fourth Revision), The Indian Roads Congress, New Delhi.

IRC:21-2000, (2000). Standard Specifications and Code of Practice for Road Bridges Section: III, Cement Concrete (Plain and Reinforced) (Third Revision), Indian Roads Congress, New Delhi, 2000.